Supporting Information

Hoadley et al. 10.1073/pnas.1117279109

SI Materials and Methods

Purification of the MM2 Peptide. cDNA encoding the FANCM MM2 peptide (residues 1218 to 1251) was cloned into a modified pGEX4T-1 plasmid (Amersham) to express a glutathione S-transferase (GST)-MM2 fusion protein in which GST and MM2 are separated by thrombin (pKH0065) or thrombin and tobacco etch virus (TEV) protease cleavage sequences (pKH0066). TEV protease cleavage separates the MM2 peptide (with a residual N-terminal Gly residue) from the remainder of the fusion protein. Multiple silent mutations were introduced for efficient *Escherichia coli* expression (pKH0069). In addition, codons for two N-terminal residues Lys-Trp were added upstream of the MM2 sequence (pKH0070). The Lys side chain is used for fluorescein isothiocyanate (FITC) labeling and the Trp is used for peptide concentration determination. The TEV-cleaved MM2 peptide sequence is: GKWEDIFDCSRDLFSVTFDLGFCSPDSDDEILEHTSD, where the underlined sequence is that of FANCM. MM2 Ala variants for FP were cloned using site-directed mutagenesis with the pKH0070 vector.

Rosetta 2 (DE3) *E. coli* cells transformed with pLysS (Novagen) and either pKH0069 or pKH0070 were grown at 30 °C in LB medium supplemented with 100 μg/mL ampicillin and 50 μg/mL chloramphenicol. At an OD_{600} of approximately 0.6 cells were induced to overexpress protein with the addition of 0.5 mM isopropyl β-D-thiogalactopyranoside for 3.5 hours. Cells were harvested with centrifugation, frozen at −80 °C, and resuspended at 4 °C in lysis buffer (50 mMTris-HCl, pH 7.5, 20% sucrose, 600 mM KCl) supplemented with 1 mM phenylmethylsulfonyl fluoride and protease-inhibitor tablets (Roche). Cells were lysed by sonication and centrifuged for 30 min at 15,000 rpm. The soluble lysate was incubated with Glutathione Sepharose 4B resin (Amersham) for 45 min, poured into a column, washed with lysis buffer, and eluted with GS4B elution buffer (25 mM Tris-HCl pH 7.5, 100 mM NaCl, 20 mM reduced glutathione). The eluate was concentrated to approximately 1.5 mL and incubated with TEV protease overnight at 4 °C. MM2 peptide was resolved on a Sephacryl S-100 column (Amersham) run at 0.2 mL/ min in S-100 buffer (10 mM Tris pH 7.5, 100 mM NaCl, 1 mM DTT, 5% glycerol). The MM2 peptides that were used in crystallization (from pKH0069) or labeled with FITC (from pKH0070) were further purified using reverse-phase HPLC and their masses confirmed with MALDI mass spectrometry. MM2 peptide variants for competition assays were not HPLC purified; these were dialyzed against 10 mM Na_2CO_3 (pH 9.3), lyophilized, and resuspended in water.

Size-Exclusion Chromatography. Uncleaved GST-MM2 used in size-exclusion chromatography (from pKH0065) was purified as described for other experiments, except that the cleavage step was omitted and the GST-MM2 was purified using the Sephacryl S-100 column. The size-exclusion experiments were performed using an analytical Sephacryl S-200 column. The GST-MM2 and RMI core complex were run individually, and then mixed at a 1:1 molar ratio and run together. Individual fractions were electrophoresed on a 15% SDS/PAGE gel.

Coimmunoprecipitations. Different chicken FANCM variants were transiently transfected into HEK293 cells. Nuclear extracts were prepared, and coimmunoprecipitation was performed using a chicken FANCM antibody (1). Actin was used as an input control.

1. Guo R, Xu D, Wang W (2009) Identification and analysis of new proteins involved in the DNA damage response network of Fanconi anemia and Bloom syndrome. *Methods* 48:72–79.

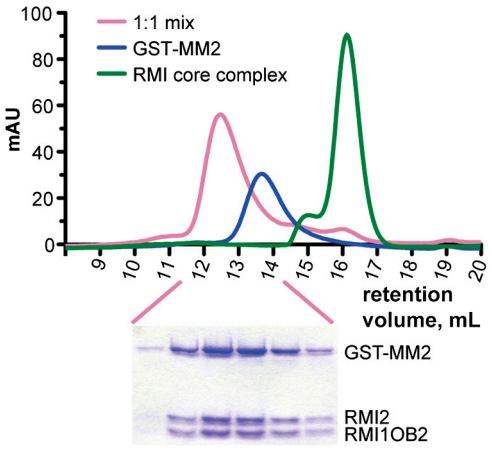

Fig. S1. Size exclusion chromatographic analysis confirms that the RMI core complex interacts with GST-MM2. The elution profiles for the RMI core complex (green), GST-MM2 (blue), and an approximately 1:1 mixture (pink) are shown. A 15% SDS/PAGE gel shown below with the peak fractions of the RMI/GST-MM2 mixture confirms that a complex forms between the RMI core complex and GST-MM2. Fractions were collected every 0.5 mL with fractions corresponding to 11.5–14 mL as shown in the gel below.

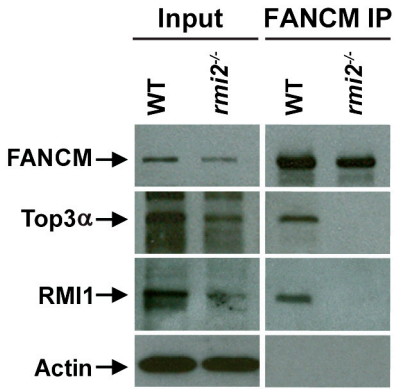

Fig. S2. The RMI subcomplex acts as a bridge between FANCM and Top3α. Protein input before coimmunoprecipitation (left), and the results of the coimmunoprecipitation with FANCM (right), shows experiments comparing wild-type and *rmi2*$^{-/-}$ chicken DT40 cells. The cell line is noted above each lane and to the left the protein probed for in Western is designated. Actin was used as a loading control.

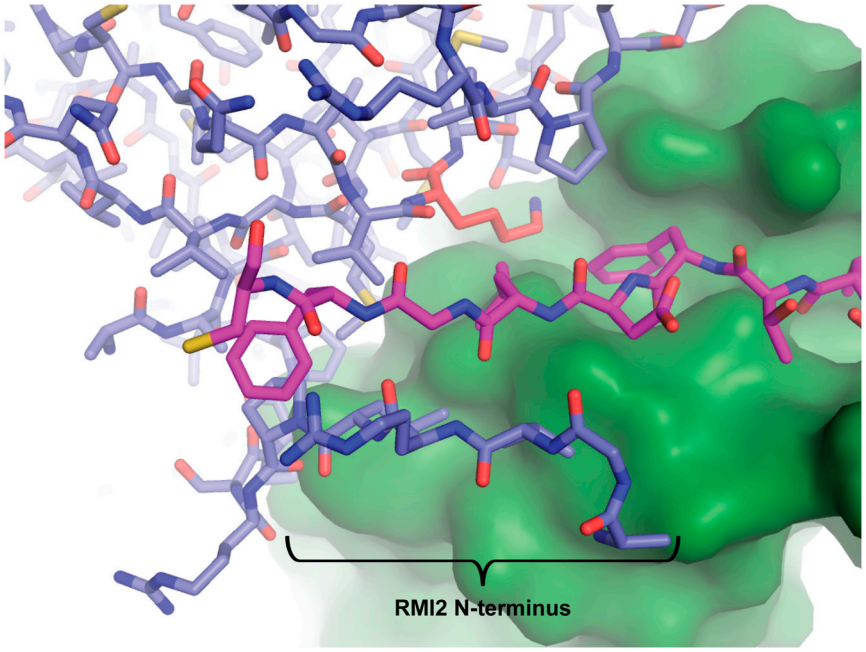

Fig. S3. The N terminus of RMI2 orders to form β-sheet interactions with the MM2 peptide. The C-terminal portion of the peptide (pink) is shown interacting with the N terminus of RMI2 (shown in blue). RMI1 is shown in green, and RMI2 Lys121 is also highlighted in red.

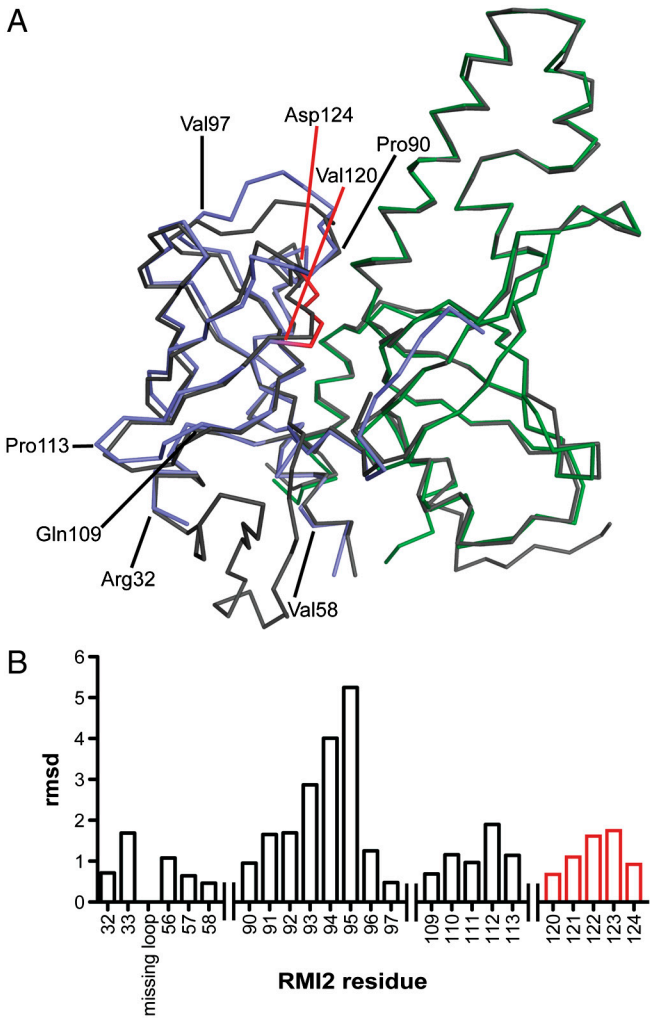

Fig. S4. Differences between the apo and MM2-bound RMI core complex. (*A*) Mainchain C$^{\alpha}$ residues from the apo (gray) and MM2-bound (RMI1 in green, RMI2 in blue) structures are aligned. Regions of movement are highlighted with lines pointing to the boundaries of these regions, and the rmsd for each of these residues is shown in *B*. The region from RMI2 residues 120–124 is shown in red. (*B*) Four regions that contained the most movement between the two structures are plotted for RMI2. The rmsd for each individual RMI2 residue is shown. "Missing loop" accounts for the loop that was only observed in the apo structure (residues 34–55 were disordered in the MM2-bound structure). The region from residues 120–124 is shown in red, as in *A*.

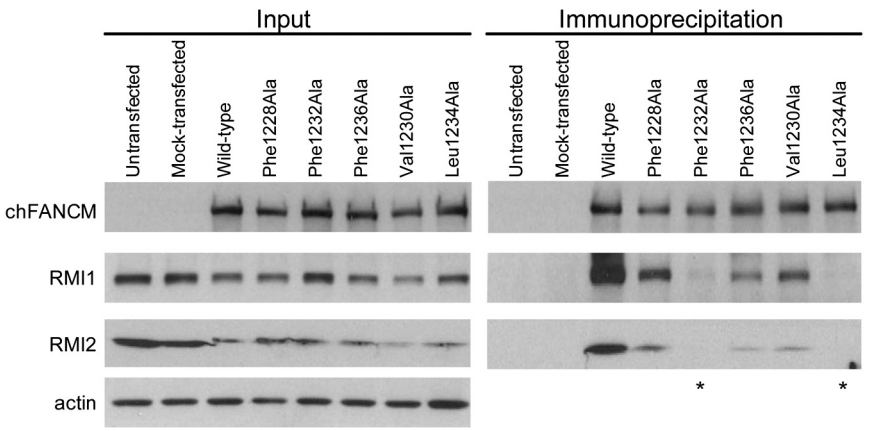

Fig. S5. Co-immunoprecipitations using various chicken FANCM variants in HEK293 cells. The left panel shows protein input before coimmunoprecipitation, and the right panel shows the results of the coimmunoprecipitation. Shown are coimmunoprecipitation experiments with Flag-tagged chicken FANCM and FANCM variants transiently transfected into HEK293 cells, followed by Western to probe for the protein shown to the left of the gel. Asterisks indicate the two residues with the most severe defect in coimmunoprecipitation.

Table S1. X-ray data collection and structure determination statistics

Data collection	
Wavelength, Å	0.97856
Resolution range (high resolution bin), Å	50-3.30 (3.36-3.30)
Space group	$I2_12_12_1$
Unit cell (a, b, c (Å))	75.3, 96.4, 99.0
(α, β, γ (°))	90, 90, 90
Completeness (high resolution bin), %	99.7 (100)
Total/unique reflections	29106/5711
Redundancy (high resolution bin)	5.1 (5.1)
$\langle I/\sigma I \rangle$ (high resolution bin)	19.9 (2.4)
R_{sym}, % (high resolution bin)*	8.1 (58.7)
Refinement	
Resolution, Å	50–3.30
R_{work}/R_{free}, %†	21.6/32.5
Rms deviations	
Bonds, Å	0.0102
Angles, °	1.38
Ramachandran statistics, %	
Most favored	84.3
Allowed	14.3
Generously allowed	1.3
Disallowed	0.0
# atoms	2,098
$\langle Bfactor \rangle$, Å^2	66.0

*$R_{sym} = \Sigma\Sigma j|Ij-\langle I \rangle|\Sigma Ij$, where Ij is the intensity measurement for reflection j and $\langle I \rangle$ is the mean intensity for multiply recorded reflections.

†$R_{work}/R_{free} = \Sigma||F_{obs}|-|F_{calc}||/|F_{obs}|$, where the working and free R factors are calculated by using the working and free reflection sets, respectively. The free R reflections (5% of the total) were held aside throughout refinement.